

PAPER • OPEN ACCESS

Assaying neural activity of children during video game play in public spaces: a deep learning approach

To cite this article: Akshay Sujatha Ravindran *et al* 2019 *J. Neural Eng.* **16** 036028

View the [article online](#) for updates and enhancements.

Recent citations

- [Characterization of the Stages of Creative Writing With Mobile EEG Using Generalized Partial Directed Coherence](#)
Jesus G. Cruz-Garza *et al*
- [Aryan Mobiny *et al*](#)

Assaying neural activity of children during video game play in public spaces: a deep learning approach

Akshay Sujatha Ravindran¹, Aryan Mobiny, Jesus G Cruz-Garza,
Andrew Paek, Anastasiya Kopteva and José L Contreras Vidal

Department of Electrical and Computer Engineering, Noninvasive Brain-Machine Interface System Laboratory, University of Houston, Houston, TX, United States of America

E-mail: asujatharavindran@uh.edu

Received 6 December 2018, revised 21 March 2019

Accepted for publication 11 April 2019

Published 8 May 2019



Abstract

Objective. Understanding neural activity patterns in the developing brain remains one of the grand challenges in neuroscience. Developing neural networks are likely to be endowed with functionally important variability associated with the environmental context, age, gender, and other variables. Therefore, we conducted experiments with typically developing children in a stimulating museum setting and tested the feasibility of using deep learning techniques to help identify patterns of brain activity associated with different conditions. *Approach.* A four-channel dry EEG-based Mobile brain-body imaging data of children at rest and during videogame play (VGP) was acquired at the Children's Museum of Houston. A data-driven approach based on convolutional neural networks (CNN) was used to describe underlying feature representations in the EEG and their ability to discern task and gender. The variability of the spectral features of EEG during the rest condition as a function of age was also analyzed. *Main results.* Alpha power (7–13 Hz) was higher during rest whereas theta power (4–7 Hz) was higher during VGP. Beta (13–18 Hz) power was the most significant feature, higher in females, when differentiating between males and females. Using data from both temporoparietal channels to classify between VGP and rest condition, leave-one-subject-out cross-validation accuracy of 67% was obtained. Age-related changes in EEG spectral content during rest were consistent with previous developmental studies conducted in laboratory settings showing an inverse relationship between age and EEG power. *Significance.* These findings are the first to acquire, quantify and explain brain patterns observed during VGP and rest in freely behaving children in a museum setting using a deep learning framework. The study shows how deep learning can be used as a data driven approach to identify patterns in the data and explores the issues and the potential of conducting experiments involving children in a natural and engaging environment.

Keywords: EEG, deep learning, CNN, video game, children, brain pattern

(Some figures may appear in colour only in the online journal)

¹ Author to whom any correspondence should be addressed.



Original content from this work may be used under the terms of the [Creative Commons Attribution 3.0 licence](https://creativecommons.org/licenses/by/3.0/). Any further distribution of this work must maintain attribution to the author(s) and the title of the work, journal citation and DOI.

1. Introduction

One of the grand challenges in cognitive-motor neuroscience is to advance the understanding of human brain dynamics in ‘action and in context’ in complex real settings. Recent developments in mobile brain-body imaging (MoBI) technology, which integrates scalp electroencephalography (EEG), and inertial movement sensors, and context-awareness, have facilitated the non-invasive, risk-free, recording and analysis of brain activity and movement with high temporal resolution in natural settings [1–5]. This technology allows researchers to study the developing brain in the pediatric population, which is critical to advance fundamental knowledge about developing patterns of neural activity in young children [6–9]. Moreover, quantitative EEG (or qEEG) measurements have diagnostic value as objective endpoints for measuring the efficacy of clinical interventions. Despite their growing importance, very little is known about the constancy and variability of qEEG measurements in the general population and specifically in the pediatric population. Studying normative neural patterns present in healthy typically-developing children and understanding its variability with demographic factors such as age and sex will support the use of qEEG in the prognosis of neurological diseases. Therefore, characterizing the normative maturation of neural patterns in the developing brain and how they are expressed in real world settings will not only advance fundamental knowledge about developmental brain dynamics, but also allow for the timely detection of neurological disorders.

Video gaming has evolved as an important social activity and is rapidly increasing in popularity. Video games are played by 97% of teenagers (between the ages of 12 and 17) and 72% of the general population as reported by the Entertainment Software Association or ESA [10]. According to a recent report, 67% of US households own a gaming device and 65% of them are home to at least one person who plays more than 3 h a week [11]. These results were evident from the video game industry reflecting net sales of \$30.4 Billion in 2016. Neurodevelopmental studies and cognitive neuroscience are now moving towards engaging wider and more diverse audiences in research. In this study, we harness the popularity of video games to capture the natural interest of the children while assaying their brain activity in a natural context (i.e. a museum) outside of the laboratory.

The main goals of this exploratory study are: (1) Acquire and quantify brain patterns in typically developing children using MoBI data while the children played Minecraft or were at rest in a museum setting; (2) Evaluate the challenges in conducting MoBI measurements from children, ‘in action and in context’; and (3) use deep learning methods to assay the patterns of neural activity (qEEG) of the participating children. To accomplish the latter, we deployed representation learning methods, which allow us to uncover representations needed for detection or classification in an unsupervised manner [12]. Specifically, we use convolutional neural networks (CNNs) to extract different high level complex abstractions as representations of the data through a learning process that is generally hierarchical in nature [13]. In the case of classifying neural

patterns, the CNN model should be able to produce representations in the deeper layers that can amplify different aspects of the input that are critical for discrimination, while suppressing irrelevant variation [14]. A model that has learned a good representation would capture the posterior distribution of the underlying explanatory factors present in the data [15]. Thus, in this study, we also aim to explore the use of CNNs for uncovering task/condition specific features learnt by the model from EEG time series data. To the best of our knowledge, this is the first MoBI dataset collected among children who voluntarily engaged into an experimental task in a public setting [16].

2. Methods

2.1. Participants

Two hundred and thirty-three (233) children (167 males/66 females) aged 6 to 16 years-old of an average age of 8.83 (SD: 2.23), participated in this experiment at the Children’s Museum of Houston during a special 1 d event after the children provided Informed Assent and the parents/guardians provided informed consent. The study was approved by the Institutional Review Board at the University of Houston.

The children were instrumented with a four-channel, dry, wireless EEG headset (Muse Interaxon, Toronto, Ontario, Canada). The headset contains seven sensors: two are positioned at the frontal region (AF7 and AF8), two are positioned at temporo-parietal region (TP9 and TP10), and the remaining sensors served as the electrical reference located near FPz. EEG data for each channel (namely, TP9, AF7, AF8, and TP10) were measured in microvolts with a sampling rate of 220 Hz. We also recorded the ‘headband status data’ for each EEG channel, which was streamed at 10 Hz. This metadata was used to determine if the headset was placed on the head properly and if the electrodes made good contact with the scalp. The EEG headset is integrated with a head accelerometer (sampled at 50 Hz), which is a basic component of MoBI systems. The Muse headset allowed for minimal setup time at the expense of whole-scalp EEG coverage.

2.2. Experimental procedure and data acquisition

The children volunteers played Minecraft (Microsoft, Washington), a popular video game where the player controls a character that can roam a large 3D procedurally-generated world. The character can explore and find resources to build and craft objects and use tools using virtual blocks within a virtual world. The game engages the player into an immersive experience where they can interact with other children playing at the museum in a shared virtual world.

A designated area at the Children’s Museum of Houston was set up with chairs facing a blank white wall as a setup to acquire data for the (baseline) rest control condition. An adjacent larger area was setup with 20 laptops arranged for playing Minecraft. Initially, the children sat in chairs facing a blank white wall and were fitted with the EEG headsets. They were asked to stare at the wall for 1 min to obtain a baseline



Figure 1. Experimental setup at the Children’s Museum of Houston. Brain waves were shown to the public as children played minecraft.

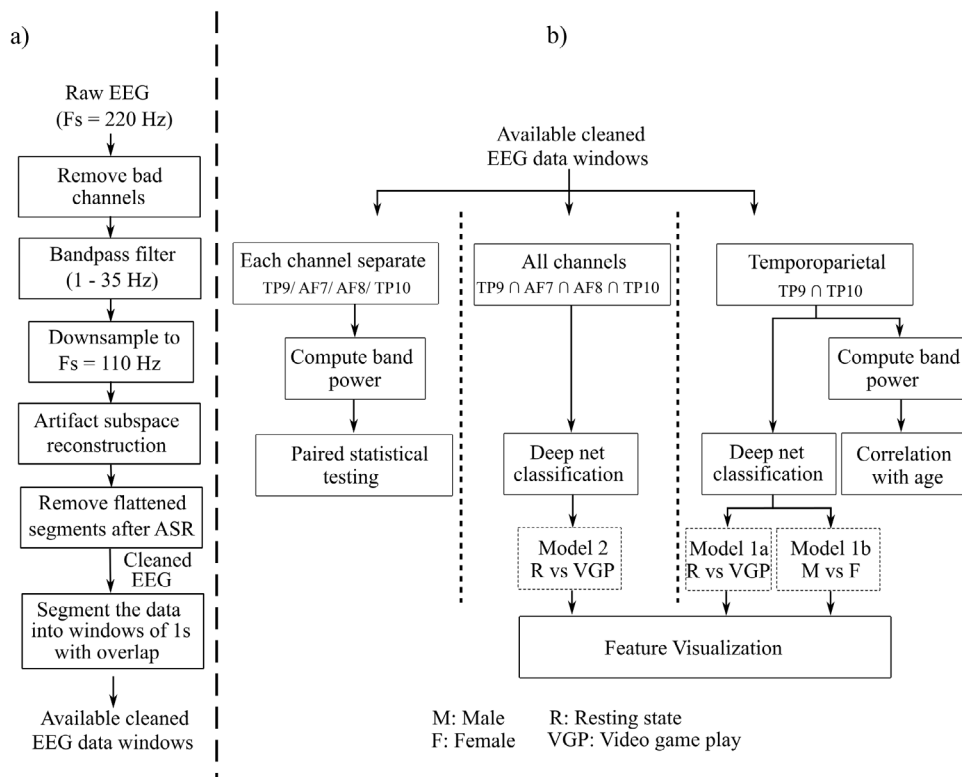


Figure 2. Analysis flowchart. Flowchart illustrating data streams and processing steps followed in the analysis.

recording of their brain activity with their eyes open. Then, they were led to the desktops where they could play Minecraft for up to 20min wherein their MoBI data would be collected as shown in figure 1. The MuseLab software included in the Muse SDK was used for visualization and data recording.

2.2.1. Signal denoising. An online notch filter was applied on EEG data while recording it (available as a consumer preset for Muse headbands) to remove the 60 Hz power line noise. Offline, channels were rejected if the headband status data was bad (>3; recommended value from the Muse company) for more than 60% of the time. We applied a 4th order, zero-phase Butterworth band-pass filter (1–35 Hz) to remove both

low and high frequency noise from EEG data. The data was then down sampled to 110 Hz. Next, artifact subspace reconstruction (ASR) [17], which is available as a plug-in through EEGLAB software [18], was used to remove short-time high-amplitude artifacts in the continuous data; from stereotypical (e.g. eye blinks or eye movements) to non-stereotypical (e.g. movement, jaw clench). A cut-off threshold of five standard deviations for identification of corrupted subspaces, a window length of 500ms with 75% overlap between two successive windows were used for ASR-based denoising. Then, signals from all channels and subjects were visually inspected using time, frequency, and time-frequency domain representations to detect and remove segments of data that did not exhibit the

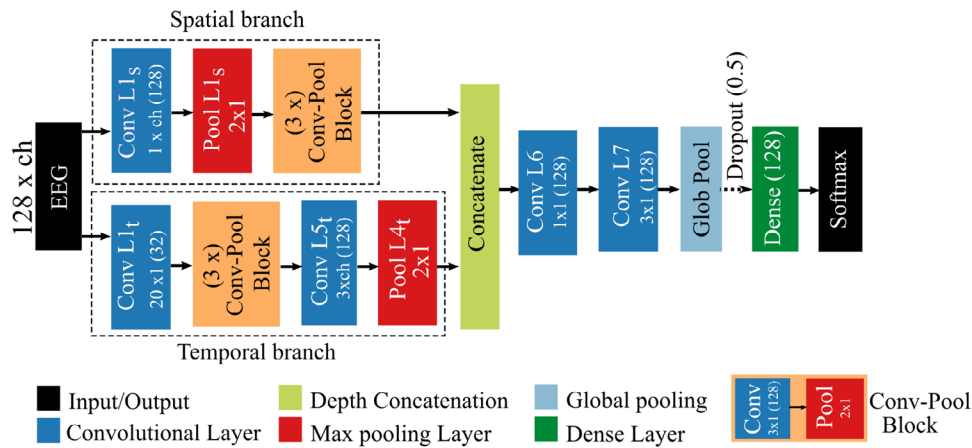


Figure 3. Network architecture. The input shape was 128 (samples) \times ch (number of channels). The output was binary and depends on the model (baseline/task or male/female).

common spectral power characteristics of EEG signal. Figure 2 depicts the data streams and the processing steps followed in the analysis.

2.2.2. CNN architecture. We used a CNN based deep network, to learn relevant features from denoised EEG data. Figure 3 illustrates the architecture of the model used in this analysis. We used an architecture inspired from that of [19] which used EEG in time series format. However, our architecture separated the spatial convolutions (across channels) and the temporal convolutions (across samples) to allow for depth in both the branches.

The input to the CNN were denoised EEG time series data (128 (samples), ~ 1.1 s) per channel. The first layer divided the model into two branches. The branching strategy is used to account for learning spatial and temporal attributes present in EEG as reported in the literature [20–26]. It is recommended to separate spatial and temporal filters in CNN for improving the interpretation of the model [19, 27] thus motivating the use of two branches that have different filter receptive fields: one learning temporal filters independent of channels and the other learning spatial filters that looks at all the channels together, which would help generate kernels that specialize in either. Similar spatial-channel specialization ‘hypothesis’ was a major factor in developing the ‘Inception’ module within deep learning architectures, wherein they decoupled the cross channel and spatial correlations to ensure they are not mapped jointly [28, 29]. Apart from depth (most EEG studies have shallow architectures [30]), proliferated paths is a major trend seen in recent years in network design that has shown promise in improvement in network performance [31]. Usage of multiple branches have shown great promise in recent years and have showed significant improvement in performance [32–35]. Taken together, these findings motivated the use of branched structure with variable filter size in the current work.

This was followed by multiple convolution-pooling layers in both branches. Each convolution filter had a filter size of (3×1) with a stride of (1×1) . The pooling layers were of size (2×1) with (2×1) strides. Padding was done for the

convolution operation to match the dimensions (‘same’ parameter in keras: ensures the output dimension is same as that of input). A $3 \times \text{ch}$ convolution layer without padding, followed by a pooling layer was added at the end of the temporal branch to make the dimensions similar for concatenating with the activation from the spatial branch, where ch is the number of channels analyzed in the network architecture. Activations from both branches were fused together using a depth concatenation layer. A 1×1 convolution layer followed this, similar to what is done in the inception model [20]. This promotes representations that combine both temporal and spatial branch activations. This was followed by another layer of 3×1 convolution without zero padding. A global average pooling layer was added to average the activation in each filter. The activation of the global average pooling layer was then fed into a fully connected dense layer with 128 hidden units with a dropout layer (probability of dropping units = 0.5) in between, to improve generalisation. A dense layer with two output nodes and softmax activation function was present at the end to give predictive probabilities for the respective classes. ReLU and ELU are the two most commonly used activation functions in deep learning models that uses EEG [30]. We selected ELU because architectures with this activation function appear to perform better for processing EEG as time series [19, 36]. It further prevents the issue associated with ‘dying ReLU’ (region corresponding to $x < 0$) seen with ReLU [37].

2.2.3. Training and testing. We trained three models sharing similar architecture as shown in figure 3, except for the number of channels used in each model. Model 1 used temporoparietal EEG data (128×2) whereas Model 2 used all four-channel data (128×4). Model 1 was further divided into two sub models. Model 1a was trained to discriminate between conditions (rest versus engaging in video game play). Model 1b was trained for classifying male versus female subjects.

Models 1a and 2 were trained to learn task relevant features for neural classification from the EEG. Model 1b was trained to classify patterns of brain activity based on sex from the

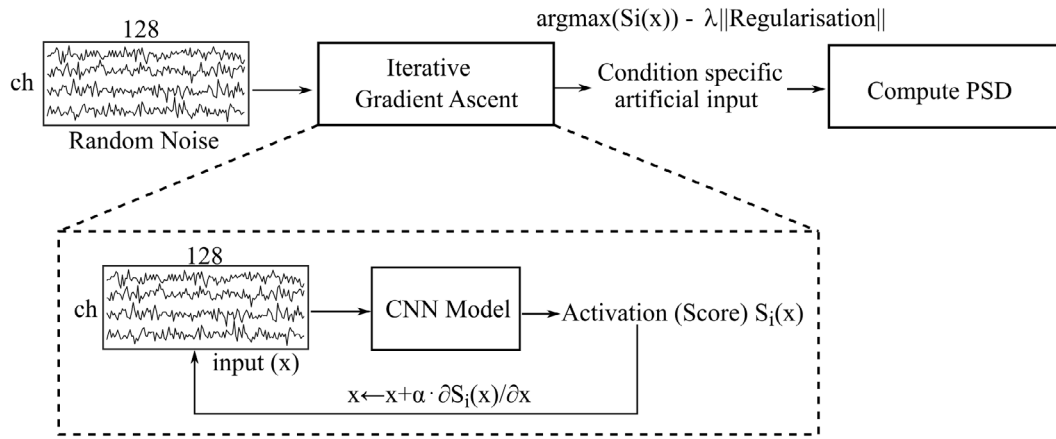


Figure 4. Visualization pipeline: PSD is computed on the artificial input generated by the activation maximization method.

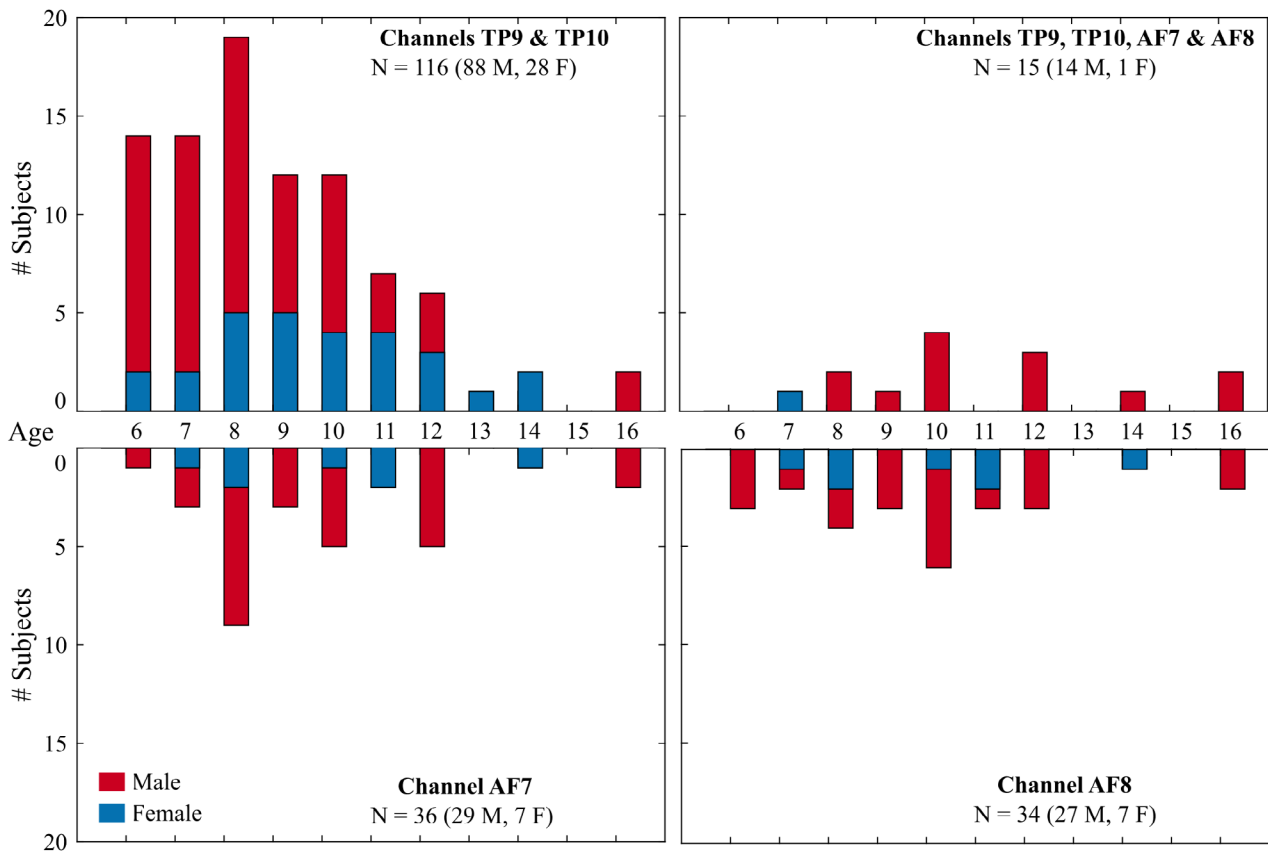


Figure 5. Demographics of participants that provided useful MoBI data from at least one, two or all four EEG channels. The age, in years, is shown on the horizontal axis, while the vertical axis shows the number of sub.

EEG data during rest condition. We did not use all four channels for sex classification due to the lower number of female subjects with all four channels as evident from figure 5.

We divided each subject’s pre-processed EEG data into intervals of training (75%) and validation (25%), without any overlap between the two. For this, we segmented validation set and training set separately first and then extracted windows from these subsets. This ensures that no single sample points would be overlapped in both training and test set. The data was then segmented into multiple 128 sample windows with variable overlap. Some of the windows were removed in the cleaning pipeline and those windows would not have been

included in training/validation sets. The amount of overlap was variable to account for the imbalance present across conditions. For instance, rest condition has more overlap as it lasts for much less time compared to video game play. So, we used 88% overlap for task and 99% overlap for rest condition. For training models 1a and 2, we used data from only male subjects as they represent the great majority of the participants and since only one female subject had all four channels that were usable.

For model 1a, we had a total of 43638 segments in video game play condition and 42422 segments of rest for the training set. A total of 13245 segments in video game play

condition and 12050 segments of EEG data during rest was used for validation. For training model 1b, we had 16623 segments of EEG data from male subjects and 15210 segments from female subjects for training. For validation, 4803 segments of males and 2768 segments of females were used. For model 2, we had a total of 7815 segments in video game play condition and 6919 segments of rest for training set. A total of 3569 segments in video game play condition and 2096 segments of rest EEG data was used for validation.

We trained the models to minimize the ‘categorical cross entropy’ loss using ‘Adam optimization’ [38] which is a first order gradient-based optimization of stochastic objective function. An L2 norm-based kernel regularization was used for all convolution filters. A dropout layer was also added between global average pooling later and the fully connected layer to improve generalization. Each model stopped training when the validation loss fails to improve for more than three consecutive epochs (early stopping condition). The model checkpoint was used to save only those weights that led to the reduction in validation loss.

In order to find the empirical chance level, the labels were shuffled randomly, and the classification accuracy on the test set for each trained model was computed separately. This was repeated for a total of 10000 times and the mean accuracy was calculated as the empirical chance level i.e. by random guess.

2.2.4. Feature learning. Since we are interested in understanding what features the deep learning model learned to discriminate between the classes, we used a visualization technique called activation maximization [39]. It can be used to generate the input which would maximally excite the final output layer nodes. Since the model is built using the one-hot-encoding basis, each node in the final layer corresponds to either of the classes. Using this technique, we initialize a vector having the same dimension as our input ($128 \times$ channels), in which each value is independently sampled from a uniform distribution (0–1). We then compute the gradient for the activation of the output node with respect to the input and take a step in the direction of the gradient. An L_p norm regularization for $p = 6$ is used to prevent input from taking very large values. We replaced the softmax activation function in the final layer to a linear function as maximization of a node with the softmax activation can be achieved by minimizing the other node which would not give optimal results. Using this gradient ascent technique, we can obtain the input data that maximally excites an output node that corresponding to different classes. The visualization pipeline using activation maximization technique is shown in figure 4. For all the models, the activation maximization technique was run to obtain the input which maximize the activation of respective output nodes/condition. Later, power spectral density (PSD) using Thomson’s multitaper method (pmtm) as implemented in Matlab (Signal Processing Toolbox Version 7.4, the MathWorks, Inc., Natick, Massachusetts, United States) was computed to check the frequency component of the signals produced. Since the methods start with random numbers, to ensure repeatability, we repeated this process 100 times for each class/output node and computed the mean and standard deviation of the PSD of the signals generated.

2.2.5. Statistical testing. The frequency-band power in delta (1–4 Hz), theta (4–7 Hz), alpha (7–12 Hz) and beta (12–30 Hz) bands were estimated by computing the one-sided PSD using the Thomson’s multitaper method (pmtm). The relative band power of each EEG segment was computed by dividing the power in each frequency band by the total power for that data segment. The mean relative power was then computed for each subject. A one-sample Kolmogorov–Smirnov test was performed to test for the normality of the EEG features at a significance level of 0.05. Since it failed the test for normality, we used the Wilcoxon signed rank sum test which is a non-parametric two-sided paired statistical test that checks if the paired difference comes from a distribution with zero median. The comparison was done at significance level of 0.05.

We limited the statistical testing for identifying differences in EEG features across condition alone (rest versus video game play) and not across gender. This is because age could also be a factor for the variation of EEG features during rest condition. Since we had only few female subjects for each age group, we did not perform the analysis across sex. For this case, the output of the deep learning visualization will be explained qualitatively based on inferences from previous studies.

2.2.6. Correlation analysis. The Pearson’s correlation coefficient was used to check for the linear relationship between different EEG spectral features with age during the rest condition in the subjects; aged 6–16. Due to the low number of subjects with frontal channel data, this analysis was limited to the temporal channels only. The analysis was done only on male subjects as we had few female subjects for each age group (figure 5). By doing so, the sex factor was statistically controlled for. For each subject, the mean value of the absolute and relative band powers in delta, theta, beta and alpha bands during the rest condition were estimated. Pearson’s correlation coefficient between absolute or relative band power and the age of the subject was then estimated. A p value < 0.05 discards the null hypothesis that there exists no linear relationship between the feature and the age.

3. Results

3.1. Evaluation of the yield of MoBI recordings in a public setting

Unfortunately, many Muse data segment recordings were lost due to several factors: (1) EEG headsets had to be recharged often and we were not able to record data from 40 subjects during these times. As a result, MoBI data was only collected from 193 subjects (out of 233 participants). From the remaining datasets, 22 datasets had empty data due to data corruption and Bluetooth connectivity issues, leaving 171 usable data sets. Some of these datasets did not have long segments of clean data due to poor placement or fitting of the device on the user’s head, particularly in the youngest children, resulting in poor electrode contact in all four channels. In addition, we could not record the rest condition in a few subjects due to non-compliance with instructions or distraction that were

Table 1. Model performance metrics: the table shows the different performance metrics on the test set data for all three models. VGP: video game play.

	Channels	Classes	Accuracy (%)	F1 score (%)	Precision (%)	Recall (%)
Model 1a	TP9 & TP10	Rest versus VGP	67.4	66.8	67.99	65.65
LOSO			67.07	66.57	66.59	66.55
Model 1b	TP9 & TP10	Male versus female	65.86	64.68	66.79	62.7
Model 2	All	Rest versus VGP	73.68	72.15	72.91	71.4

typical of crowded places such as a museum (18 subjects ~8%). After rejecting these subjects, we retained a total of 117 (88 M, 29 F) subjects, which had usable MoBI segments in at least a single channel after the denoising pipeline shown in figure 2(a). The distribution of available data across each channel is shown in figure 5.

3.2. Analysis of head acceleration

We compared the distribution of mean band-pass filtered ((0.1–10 Hz), 4th-order Butterworth filter) head accelerations during game playing (VGP) and rest conditions (figure 6) associated with the EEG windows retained after our preprocessing (denoising) pipeline shown in figure 2(a). As expected, head acceleration was very small and significantly lower during Rest condition compared to the VGP condition ($p < 0.05$) using t -test. Note that for the VGP group, all retained EEG windows consisted of data from male participants only. Thus, effects of gender on head acceleration were computed only for the rest condition that was comprised of data from both boys and girls.

3.3. Model performance

The proposed CNN-based models were implemented in python 3.6 using Keras [40] 2.1.5 wrapper with TensorFlow backend [41]. All three models were trained separately until the validation loss stopped improving for three successive epochs. The parameters that yielded good performance were empirically selected through multiple combinations. The performance metrics such as classification accuracy, F1 score, recall score and precision score for all the models have been summarized in table 1. The empirical chance levels obtained were ($50.2\% \pm 0.3\%$) for model 1a. ($56.0\% \pm 0.54\%$) for 1b and ($55.1\% \pm 0.51\%$) for model 2. The models did not overfit to the training data as evident from the smooth reduction in both the training and validation loss throughout (figure 7(b)). To further show that the model can generalize well across unseen data/subjects, we performed the leave one subject out (LOSO) validation strategy for the model 1a. That uses EEG from temporoparietal channels. Validation using LOSO strategy yielded a mean validation accuracy of 67.07% (figure 7(c)). This further shows the potential of deep networks being able to generalize well across subject.

3.4. Feature learning

We used the visualization toolkit, keras-vis, to implement the activation maximization technique. Figure 7(a) shows the

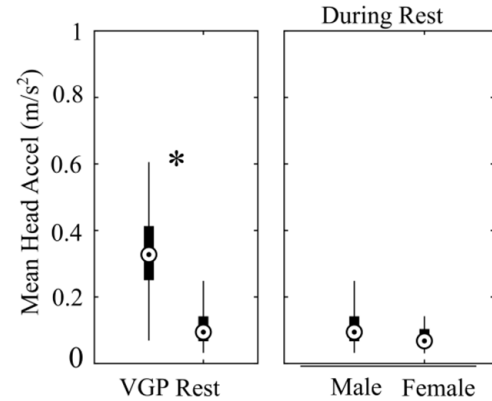


Figure 6. Head acceleration distribution. (Left) The distribution of mean head acceleration of the denoised windows used in the analysis during video game play and rest conditions. (Right) Distribution of mean head acceleration during rest condition, for male versus female participants. * Indicates a statistically significant difference between the two groups ($p < 0.05$).

average PSD with standard deviation for the artificial input generated by the activation maximization technique. For model 1a, which discriminates between rest and video game playing conditions, a decrease in theta band power relative to the video game play condition was found during the rest state condition. Also, a large peak is observed in the alpha band during the rest condition, which is absent during the video game play.

Similarly, for model 1b, which learnt to discriminate between male and female participants in the rest conditions, the visualization method yielded the results shown in figure 7(a). Beta power between 13 and 18 Hz was the most discriminative feature in EEG for sex classification. There was higher 13–18 Hz beta power in females compared to males.

For Model 2, which used all four EEG channels, the visualization step identified peaks in the alpha band during the rest condition as seen in figure 7(a). There exists another large peak in the theta band during video gameplay compared to a suppression during rest condition. Certain small peaks in the beta band, particularly in the frontal channels, were also observed during the video game play condition.

3.5. Statistical testing

A paired statistical test was performed to check for significant difference in spectral features of input EEG between rest and video game playing conditions. As seen in figure 7(d), the relative theta power was statistically significantly different between rest and video game play conditions in both temporoparietal channels ($p < 0.01$). It was found to be higher during

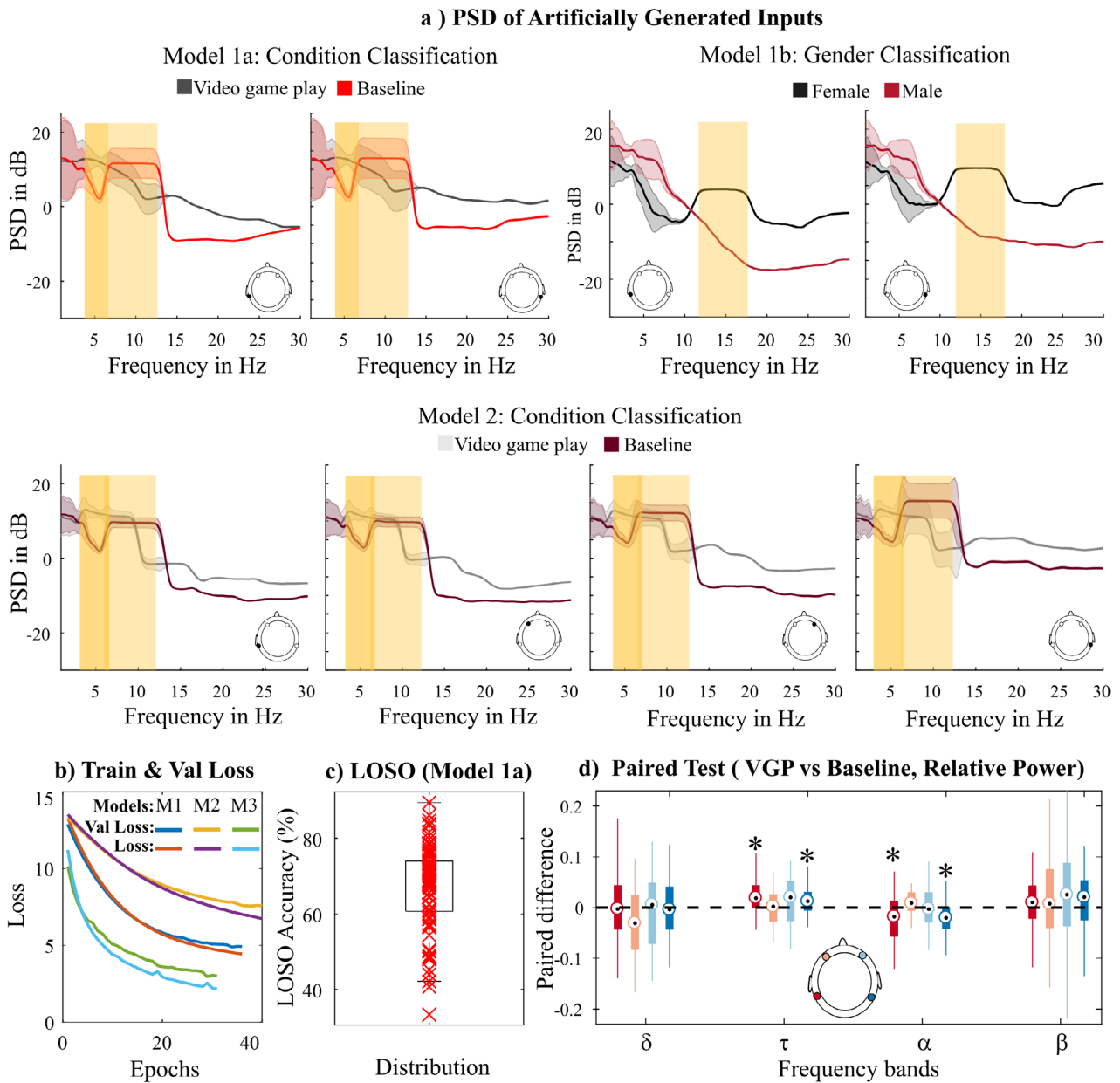


Figure 7. Feature learning using deep network. (a) PSD (mean and standard deviation) of the input, which were artificially generated by the respective models for each class. The yellow shaded region indicates the regions of interesting findings from the deep network. (b) Training and validation loss for all three models with increasing epochs. (c) Distribution of LOSO validation accuracy for model 1a. (d) Distribution of the difference in relative band power in the original EEG across rest and video game playing (VGP) condition. * Indicates statistically significant difference at $p < 0.01$.

video game play relative to rest condition. Similarly, relative alpha power was found to be statistically significant in TP9 and TP10 for $p < 0.01$; higher during the rest condition. Even though relative beta power was not found to be significantly different across conditions, the values tend to be higher during video game play compared to rest condition, particularly in the AF8 electrode.

3.6. Correlation analysis: EEG features versus age

The correlation analysis was conducted to check for a linear relationship between the EEG spectral features and the age of children. A significant negative correlation ($p < 0.05$) for the

absolute band powers for theta ($r = -0.36$ in TP9 & -0.32 in TP10) and alpha ($r = -0.23$ in TP9 & -0.30 in TP10) band was observed in both temporo-parietal channels. Only the TP9 channel showed significant negative correlation in delta band ($r = -0.36$ in TP9 & -0.16 in TP10). Even though beta power reduced with age ($r = -0.12$ in TP9 & -0.20 in TP10), the correlation was not significant at $p < 0.05$. In general, all absolute band power across frequency bands reduced with age. Figure 8 shows the general trend of these features for the age groups 6 to 12 years old.

Among the relative power terms only the relative delta band power ($r = -0.30$) in the TP9 channel showed significant negative correlation for $p < 0.05$. Even though not

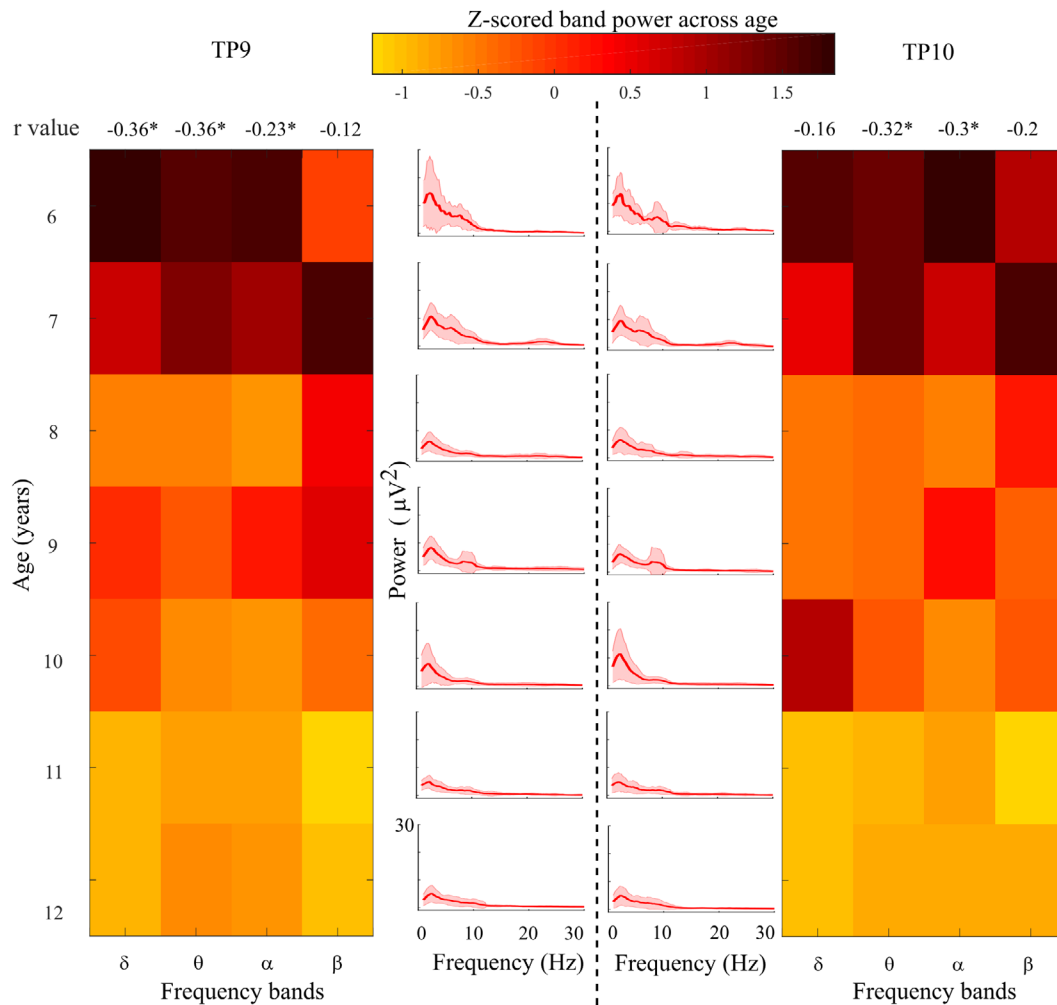


Figure 8. Correlation analysis. The colored box corresponds to the standardized mean power for each age group. The power is standardized per frequency band for visualization purpose alone. The colored PSD corresponds to the mean PSD with the standard deviation (shaded) across subjects. The correlation coefficient (r) was computed for the age groups 6 to 16 years old; *: $p < 0.05$.

statistically significant at the significance level of 0.05, the relative power in the upper frequency bands, alpha ($r = 0.23$ in TP9 & $r = 0.05$ in TP10) and beta ($r = 0.18$ in TP9 & $r = 0.12$ in TP10) correlated positively with age, and the lower frequency bands, delta ($r = -0.3$ in TP9 & $r = -0.1$ in TP10) and theta ($r = -0.15$ in TP9 & $r = -0.15$ in TP10) correlated negatively.

4. Discussion

In a single day we recruited 233 children for our MoBI study at the Children’s Museum of Houston. We were limited in the number of participants we could enroll in our study due to the limited availability of both EEG headsets and exhibit room space at the museum. Nevertheless, the excellent public response to our study supports the use of gamification for conducting research in public spaces. Games that elicit certain cognitive events in a targeted fashion could be designed and deployed to collect data from a larger number of subjects in the future. However, among the 233 subjects, the yield from the MoBI recordings was only 50% (that, is 117 subjects) as many children did not have reliable recordings from all four

dry EEG channels. This yield was in part due to fitting problems as the Muse headsets were designed primarily for the adult population, and thus, they have not accounted for the variability of form and skull size in young children. This could be the reason for poor contact in multiple channels found in children (particularly the frontal channels), leading to data loss.

4.1. Rest condition

Using a deep learning model, we explored methods to identify task and sex specific features from the EEG data. All the models performed well above the chance level even with only two channels. As seen from table 1, the classification accuracies increased with the number of channels (model 1a versus model 2) available for classification. Using the visualization technique in models 1a and 2, we identified alpha power to be the dominant feature during the rest condition, which was expected. This phenomenon of exhibiting larger alpha power during the rest condition has been reported frequently in multiple studies and is associated with the brain entering an idling state [42–45].

4.2. Videogame condition

We also observed a theta peak during video game play, which was attenuated during the rest condition. An increase in theta band power is thought to reflect the increase in cortical activation due to high mental effort and attention [46, 47]. This increase has been widely reported in video game play studies [48–50]. Similarly, beta activity, particularly in the frontal channels have been reported to be associated with alert attentiveness and goal directed actions [51–54]. Our observations from the deep network visualization method agrees with these prior findings.

Similarly, model 1b, which was trained to discriminate based on sex, showed larger beta power (12–18 Hz) for females as the most distinguishing feature. Multiple prior studies have identified similar observations in which beta power has been reported to be higher in female subjects compared to male [55–57]. For example, in a similar study that investigated the EEG during rest condition from 1308 subjects, beta activity was found to be the most distinctive attribute in discriminating between male and female subjects [57]. This also agrees with what we observed.

As additional validation of our findings using the visualization method for deep networks, we performed a statistical analysis using a non-parametric paired test to see whether the changes in relative band power present in the real data were indeed in agreement with what was visualized by the deep net. Across conditions, it is indeed found that the relative alpha power is higher in rest compared to video game play. The relative theta band power was higher during video game play compared to rest, which is again in agreement with the visualization results. However, this was statistically significant only in the temporal-parietal channels and not in the frontal channels. This could be associated with the lower number of subjects with frontal channel EEG. Further analysis is needed with a greater number of subjects to validate this finding. The beta power was also observed to be higher during video game play compared to the rest condition, but this did not reach statistical significance.

We also investigated the age-related changes in spectral features in EEG in the temporo-parietal channels. Similar to prior research work, we observed that absolute power decreased with age in all frequency bands, particularly in the slower frequency bands [50, 58–62]. The general trend observed in this study were again in agreement with prior research, which associates the reduction in slow wave activity with the reduction in gray matter as we develop/mature [59–63]. The relative power had a trend of correlating negatively with age for delta and theta bands while the faster bands like alpha and beta correlated positively with age [50, 59–63]. This trend is consistent with what is observed in previous studies. However only the theta band in TP9 was found to be statistically significant in our analysis.

4.3. Conclusion

In summary, we explored the possibility and challenges associated with conducting experiments with children in a

stimulating complex public environment. We also explored the feasibility of using deep learning techniques to help identify relevant patterns of brain activity associated with different conditions: rest versus video game play, and male versus female. This approach could be an efficient tool to be used in studies to uncover patterns from the data. Overall, the current study contributes to a better understanding of how deep learning can be used as a data driven approach to identify patterns in your data and explored the issues and the potential of conducting experiments involving children in a natural and engaging environment. The data analyzed in this study is available to the scientific community through IEEE Dataport [64].

Acknowledgments

This research was supported in part by the National Science Foundation Award BCS 1533691. We acknowledge the logistical support of all members of the Noninvasive Brain–Machine Interface Systems Laboratory at the University of Houston, who assisted with the data collection at the Children’s Museum of Houston. This work could not have been done without the support of Julia Banda, Gretchen Schmaltz, and Neelam Damani, Director of Gallery Education at the Children’s Museum of Houston. This work was completed in part with resources provided by the Core facility for Advanced Computing and Data Science at the University of Houston.

The authors have confirmed that any identifiable participants in this study have given their consent for publication

Data availability statement

The datasets analyzed for this study can be found in the IEEE Dataport (<https://doi.org/10.21227/H23W88>).

Conflict of interest

All financial, commercial or other relationships that might be perceived by the academic community as representing a potential conflict of interest must be disclosed. If no such relationship exists, authors will be asked to confirm the following statement:

The authors declare that the research was conducted in the absence of any commercial or financial relationships that could be construed as a potential conflict of interest.

ORCID iDs

Akshay Sujatha Ravindran  <https://orcid.org/0000-0001-7213-9587>

Aryan Mobiny  <https://orcid.org/0000-0002-6040-4264>

Jesus G Cruz-Garza  <https://orcid.org/0000-0002-8440-6416>

Andrew Paek  <https://orcid.org/0000-0001-5467-9280>

José L Contreras Vidal  <https://orcid.org/0000-0002-6499-1208>

References

- [1] Cruz-Garza J G *et al* 2017 Deployment of mobile EEG technology in an art museum setting: evaluation of signal quality and usability *Frontiers Hum. Neurosci.* **11** 527
- [2] Kontson K, Megjhani M, Brantley J A, Cruz-Garza J G, Nakagome S, Robleto D, White M, Civillico E and Contreras-Vidal J L 2015 ‘Your brain on art’: emergent cortical dynamics during aesthetic experiences *Frontiers Hum. Neurosci.* **9** 626
- [3] Herrera-Arcos G *et al* 2017 Modulation of neural activity during guided viewing of visual art *Frontiers Hum. Neurosci.* **11** 581
- [4] Hashemi A, Pino L J, Moffat G, Mathewson K J, Aimone C, Bennett P J, Schmidt L A and Sekuler A B 2016 Characterizing population EEG dynamics throughout adulthood *ENEURO* **3** ENEURO.0275-16.2016
- [5] Kovacevic N, Ritter P, Tays W, Moreno S and McIntosh A R 2015 ‘My virtual dream’: collective neurofeedback in an immersive art environment *PLoS One* **10** e0130129
- [6] Benasich A A, Gou Z, Choudhury N and Harris K D 2008 Early cognitive and language skills are linked to resting frontal gamma power across the first 3 years *Behav. Brain Res.* **195** 215–22
- [7] Tierney A, Strait D L, O’Connell S and Kraus N 2013 Developmental changes in resting gamma power from age three to adulthood *Clin. Neurophysiol.* **124** 1040–2
- [8] Vlahou E L, Thurm F, Kolassa I T and Schlee W 2014 Resting-state slow wave power, healthy aging and cognitive performance *Sci. Rep.* **4** 5101
- [9] Zappasodi F, Marzetti L, Olejarczyk E, Tecchio F and Pizzella V 2015 Age-related changes in electroencephalographic signal complexity *PLoS One* **10** e0141995
- [10] Entertainment Software Association 2017 Essential facts 2017 *ESA Report 2017* (www.theesa.com/wp-content/uploads/2017/04/EF2017_FinalDigital.pdf) accessed 24/04/2019
- [11] Lenhart A, Kahne J, Middaugh E, Macgill A, Evans C and Vitak J 2008 *Teens’ Gaming Experiences are Diverse and Include Significant Social Interaction and Civic Engagement* (Washington, DC: Pew Internet & American Life Project)
- [12] Bengio Y, Courville A and Vincent P 2013 Representation learning: a review and new perspectives *IEEE Trans. Pattern Anal. Mach. Intell.* **35** 1798–828
- [13] Krauledat M, Tangermann M, Blankertz B and Müller K R 2008 Towards zero training for brain–computer interfacing *PLoS One* **3** e2967
- [14] LeCun Y, Bengio Y and Hinton G 2015 Deep learning *Nature* **521** 436
- [15] Bengio Y, Courville A C and Vincent P 2012 Unsupervised feature learning and deep learning: a review and new perspectives, CoRR (arXiv:1206.5538)
- [16] Wolpaw J R 2007 Brain–computer interfaces as new brain output pathways *J. Physiol.* **579** 613–9
- [17] Mullen T, Kothe C, Chi Y M, Ojeda A, Kerth T, Makeig S, Cauwenberghs G and Jung T P 2013 Real-time modeling and 3D visualization of source dynamics and connectivity using wearable EEG 2013 *35th Annual Int. Conf. IEEE Eng. Med. Biol. Soc. (EMBC) (3 July 2013)* (IEEE) pp 2184–7
- [18] Delorme A and Makeig S 2004 EEGLAB: an open source toolbox for analysis of single-trial EEG dynamics including independent component analysis *J. Neurosci. Methods* **134** 9–21
- [19] Schirrneister R T *et al* 2017 Deep learning with convolutional neural networks for EEG decoding and visualization *Hum. Brain Mapp.* **38** 5391–420
- [20] Canolty R T, Edwards E, Dalal S S, Soltani M, Nagarajan S S, Kirsch H E, Berger M S, Barbaro N M and Knight R T 2006 High gamma power is phase-locked to theta oscillations in human neocortex *Science* **313** 1626–8
- [21] Nunez P L, Wingeier B M and Silberstein R B 2001 Spatial-temporal structures of human alpha rhythms: theory, microcurrent sources, multiscale measurements, and global binding of local networks *Hum. Brain Mapp.* **13** 125–64
- [22] Nunez P L 1989 Generation of human EEG by a combination of long and short range neocortical interactions *Brain Topogr.* **1** 199–215
- [23] Schirrneister R, Gemein L, Eggenesperger K, Hutter F and Ball T 2017 Deep learning with convolutional neural networks for decoding and visualization of EEG pathology 2017 *IEEE Signal Processing in Medicine and Biology Symp. (SPMB) (2 December 2017)* (IEEE) pp 1–7
- [24] Olejniczak P 2006 Neurophysiologic basis of EEG *J. Clin. Neurophysiol.* **23** 186–9
- [25] Jackson A F and Bolger D J 2014 The neurophysiological bases of EEG and EEG measurement: a review for the rest of us *Psychophysiology* **51** 1061–71
- [26] Buzsáki G 2006 *Rhythms of the Brain* (Oxford: Oxford University Press)
- [27] Cecotti H and Gräser A 2011 Convolutional neural networks for P300 detection with application to brain–computer interfaces *IEEE Trans. Pattern Anal. Mach. Intell.* **33** 433–45
- [28] Chollet F 2017 Xception: deep learning with depthwise separable convolutions *Proc.—30th IEEE Conf. on Computer Vision and Pattern Recognition (CVPR 2017)* pp 1800–7
- [29] Szegedy C *et al* 2015 Going deeper with convolutions *Proc. IEEE Computer Society Conf. on Computer Vision and Pattern Recognition* pp 1–9
- [30] Craik A, He Y and Contreras-Vidal J L 2019 Deep learning for electroencephalogram (EEG) classification tasks: a review *J. Neural Eng.* **16** 031001
- [31] Smith L N and Topin N 2016 Deep convolutional neural network design patterns (arXiv:1611.00847)
- [32] Zhang X, Li Z, Loy C C and Lin D 2017 PolyNet: a pursuit of structural diversity in very deep networks *Proc.—30th IEEE Conf. on Computer Vision and Pattern Recognition (CVPR 2017)* pp 3900–8
- [33] Szegedy C, Ioffe S, Vanhoucke V and Alemi A A 2017 Inception-v4, inception-resnet and the impact of residual connections on learning *31st AAAI Conf. on Artificial Intelligence (12 February 2017)*
- [34] Li B, Luo H, Zhang H, Tan S and Ji Z 2017 A multi-branch convolutional neural network for detecting double JPEG compression (arXiv:1710.05477)
- [35] Ioannou Y, Robertson D, Zikic D, Kontschieder P, Shotton J, Brown M and Criminisi A 2016 Decision forests, convolutional networks and the models in-between (arXiv:1603.01250)
- [36] Lawhern V J, Solon A J, Waytowich N R, Gordon S M, Hung C P and Lance B J 2018 EEGNet: a compact convolutional neural network for EEG-based brain–computer interfaces *J. Neural Eng.* **15** 056013
- [37] Clevert D A, Unterthiner T and Hochreiter S 2015 Fast and accurate deep network learning by exponential linear units (elus) (arXiv:1511.07289)
- [38] Kingma D P and Ba J 2014 Adam: a method for stochastic optimization (arXiv:1412.6980)
- [39] Erhan D, Bengio Y, Courville A and Vincent P 2009 Visualizing higher-layer features of a deep network

- ICML 2009 Workshop on Learning Feature Hierarchies (University of Montreal, Montréal, Canada) vol 1341, p 1
- [40] Chollet F 2018 Keras: the python deep learning library, Astrophysics Source Code Library
- [41] Abadi M *et al* 2016 Tensorflow: a system for large-scale machine learning *12th USENIX Symp. on Operating Systems Design and Implementation (OSDI 2016)* pp 265–83
- [42] Tenke C E, Kayser J, Abraham K, Alvarenga J E and Bruder G E 2015 Posterior EEG alpha at rest and during task performance: comparison of current source density and field potential measures *Int. J. Psychophysiol.* **97** 299–309
- [43] Barry R J, Clarke A R, Johnstone S J and Brown C R 2009 EEG differences in children between eyes-closed and eyes-open resting conditions *Clin. Neurophysiol.* **120** 1806–11
- [44] Klimesch W 2012 Alpha-band oscillations, attention, and controlled access to stored information *Trends Cogn. Sci.* **16** 606–17
- [45] Li L 2010 The differences among eyes-closed, eyes-open and attention states: an EEG study *2010 6th Int. Conf. on Wireless Communications Networking and Mobile Computing (WiCOM) (23 September 2010)* (IEEE) pp 1–4
- [46] Salminen M and Ravaja N 2008 Increased oscillatory theta activation evoked by violent digital game events *Neurosci. Lett.* **435** 69–72
- [47] Naumann L, Schultze-Kraft M, Dähne S and Blankertz B 2017 Prediction of difficulty levels in video games from ongoing EEG *Lecture Notes in Computer Science (Lecture Notes in Artificial Intelligence and Lecture Notes in Bioinformatics)* (Cham: Springer) pp 125–36
- [48] Sheikholeslami C, Yuan H, He E J, Bai X, Yang L and He B 2007 A high resolution EEG study of dynamic brain activity during video game play *Annual Int. Conf. IEEE Eng. Med. Biol. Soc.* pp 2489–91
- [49] He E J, Yuan H, Yang L, Sheikholeslami C and He B 2008 EEG spatio-spectral mapping during video game play *2008 Int. Conf. on Information Technology and Applications in Biomedicine (30 May 2008)* (IEEE) pp 346–8
- [50] Pellouchoud E, Smith M E, McEvoy L and Gevins A 1999 Mental effort-related EEG modulation during video-game play: comparison between Juvenile subjects with epilepsy and normal control subjects *Epilepsia* **40** 38–43
- [51] Salminen M and Ravaja N 2007 Oscillatory brain responses evoked by video game events: the case of super monkey ball *Cyberpsychol. Behav.* **10** 330–8
- [52] Malik A S, Osman D A, Pauzi A A and Khairuddin R H 2012 Investigating brain activation with respect to playing video games on large screens *4th Int. Conf. on Intelligent and Advanced Systems (ICIAS2012) (12 Jun 2012)* vol 1 (IEEE) pp 86–90
- [53] Davidson R J, Jackson D C and Larson C L 2000 Human electroencephalography *Handbook of Psychophysiology* (Cambridge: Cambridge University Press) pp 27–52
- [54] Takahashi N, Shinomiya S, Mori D and Tachibana S 1997 Frontal midline theta rhythm in young healthy adults *Clin. EEG Neurosci.* **28** 49–54
- [55] Dimpfel W 2015 V20. Gender differences in the quantitative EEG in relaxed states and during cognitive or emotional challenges *Clin. Neurophysiol.* **126** e76
- [56] Aslanyan E V, Kiroy V N, Bakhtin O M, Minyaeva N R, Lazurenko D M and Tambiev A E 2017 Gender differences in spontaneous and evoked activities of the human brain *Hum. Physiol.* **43** 644–52
- [57] Putten M J, Olbrich S and Arns M 2018 Predicting sex from brain rhythms with deep learning *Sci. Rep.* **8** 3069
- [58] Gasser T, Verleger R, Bächer P and Sroka L 1988 Development of the EEG of school-age children and adolescents. I. Analysis of band power *Electroencephalogr. Clin. Neurophysiol.* **69** 91–9
- [59] Clarke A R, Barry R J, McCarthy R and Selikowitz M 2001 Age and sex effects in the EEG: development of the normal child *Clin. Neurophysiol.* **112** 806–14
- [60] Gmehlin D *et al* 2011 Individual analysis of EEG background-activity within school age: impact of age and sex within a longitudinal data set *Int. J. Dev. Neurosci.* **29** 163–70
- [61] Barriga-Paulino C I, Flores A B and Gómez C M 2011 Developmental changes in the EEG rhythms of children and young adults: analyzed by means of correlational, brain topography and principal component analysis *J. Psychophysiol.* **25** 143–58
- [62] Miskovic V *et al* 2015 Developmental changes in spontaneous electrocortical activity and network organization from early to late childhood *NeuroImage* **118** 237–47
- [63] Niemarkt H J *et al* 2011 Maturational changes in automated EEG spectral power analysis in preterm infants *Pediatr. Res.* **70** 529–34
- [64] Ravindran A S, Cruz-Garza J G, Kopteva A, Paek A, Mobiny A, Hernandez Z and Contreras-Vidal J L 2017 Multi-modal mobile brain-body imaging (MoBI) dataset for assaying neural and head movement responses associated with creative video game play in children, IEEE Dataport (Available from: <https://doi.org/10.21227/H23W88>)